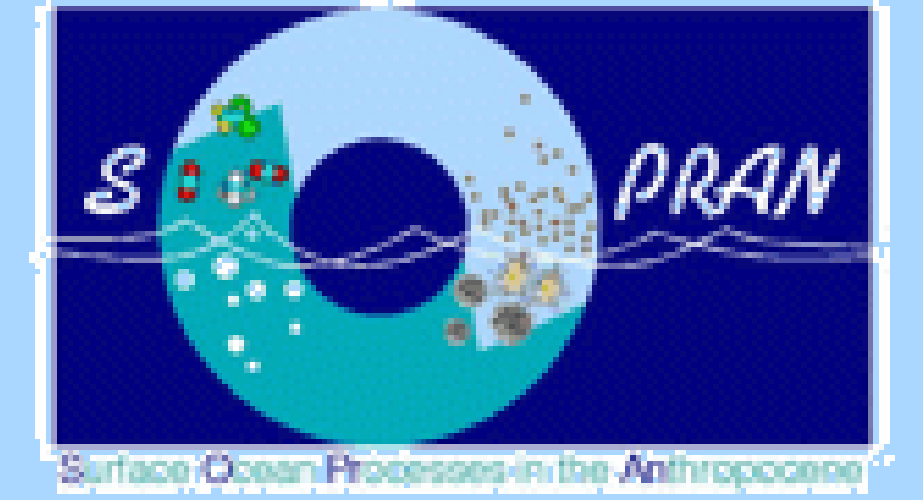


# Key controls on the cycle of organic Fe-binding ligands in a 3D model



Ying Ye, Christoph Völker, Dieter A. Wolf-Gladrow  
Alfred Wegener Institute, Helmholtz Centre for Polar and Marine Research  
Ying.Ye@awi.de



## Knowledge on organic ligands and model improvements

Most dissolved iron (DFe) in the ocean is bound to organic ligands, which regulate the reactive fraction of DFe available for particle adsorption, and thus its residence time. New insights into the sources and fate of these ligands have been gained over the last decade and patterns of spatial variability are beginning to emerge (Fig. 1). Assumptions on ligand abundance are therefore critical for biogeochemical models including iron. Instead of fixing organic ligands to an observed mean concentration, Völker and Tagliabue (2014) firstly implemented a mechanistic description of ligand dynamics in two 3D models (PISCES and RecoM). In this study, a series of sensitivity experiments has been done with REcoM dealing with the uncertainty in some parameter values describing ligand production and loss. Furthermore, we have explored the impact of changing parameter values on Fe distribution.

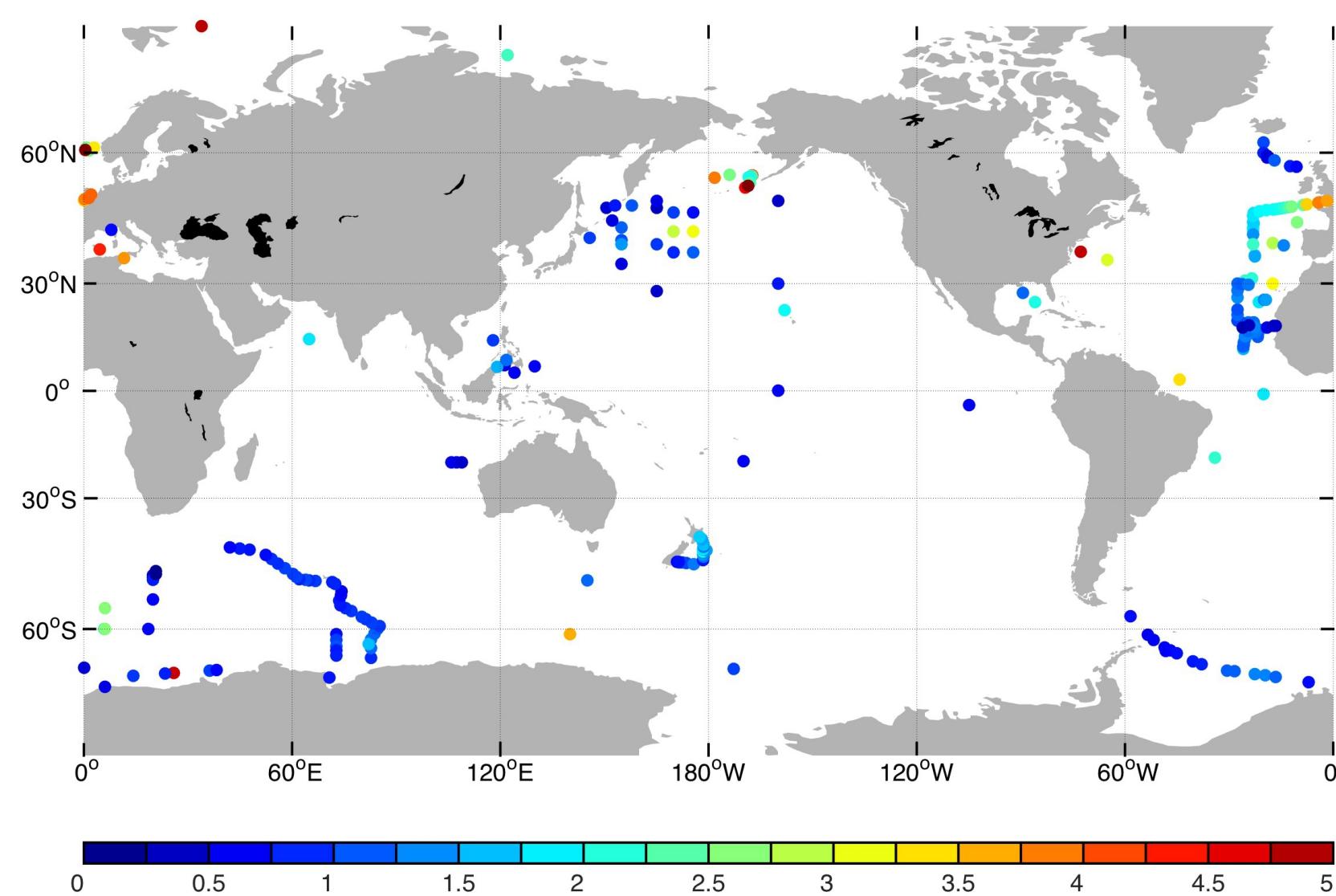


Fig. 1 Observed total ligand concentration in the upper 50m (nM). We collected data from published ligand measurements with electrochemical methods and Fe(III) solubility measurements which are interpreted as a measure for ligand abundance.

## Modelled processes and parameter values

The biogeochemical model used in this study is RecoM-2 (Hauck et al., 2013) coupled with MITgcm (Marshall et al., 1997). It is a NPZD-type model with two phytoplankton size classes. We use a horizontal resolution of  $2^\circ \times 2^\circ \cos\phi$  and 30 vertical layers. The ligand cycle is described based on Ye et al. (2009) and Völker and Tagliabue (2014), considering the following processes:

- 1) Ligand release through POC remineralisation with a constant ligand:carbon ratio (**lig:C**);
- 2) Ligand production by living organisms with a constant ligand:DOC ratio;
- 3) Microbial degradation of ligands once with a fixed and once a variable timescale ( $\tau$ ) making the degradation faster at higher ligand concentrations;
- 4) Photochemical degradation of ligands depending on light, ligand concentration and degradation rate constant ( $k_{ph}$ );
- 5) Ligand loss by phytoplankton uptake of organically complexed Fe;
- 6) Aggregation of a fraction of ligands with sinking particles.

Tab. 1 Parameter values and correlation coefficients for surface and deep water (runs shown in this poster).

Run	lig:C * 10 <sup>-3</sup>	$k_{ph}$ (10 <sup>-4</sup> W <sup>-1</sup> m <sup>2</sup> d <sup>-1</sup> )	$\tau$ (year)	corr. coeff. (s)	corr. coeff. (d)
n04	0.010	0.047 (1x)	400	0.09	0.54
n05	0.025	0.047 (1x)	400	0.03	0.54
n06	0.050	0.047 (1x)	400	0.02	0.54
n07	0.100	0.047 (1x)	400	0.02	0.54
n13	0.010	0.465 (10x)	400	0.08	0.35
n14	0.010	0.930 (20x)	400	0.11	0.28
n17	0.010	0.465 (10x)	200	0.14	0.39
vartau5	0.050	1.000 (~20x)	variable	0.40	0.14

## I. Changing the lig:C ratio

Increasing the lig:C ratio leads to clearly higher concentrations of ligands throughout the water column (Fig. 2). Deep water distribution of ligand has a relatively high model-data agreement around 54% (Tab. 1), indicating that the remineralisation source, microbial degradation and ocean circulation mainly control the ligand cycling in deep waters.

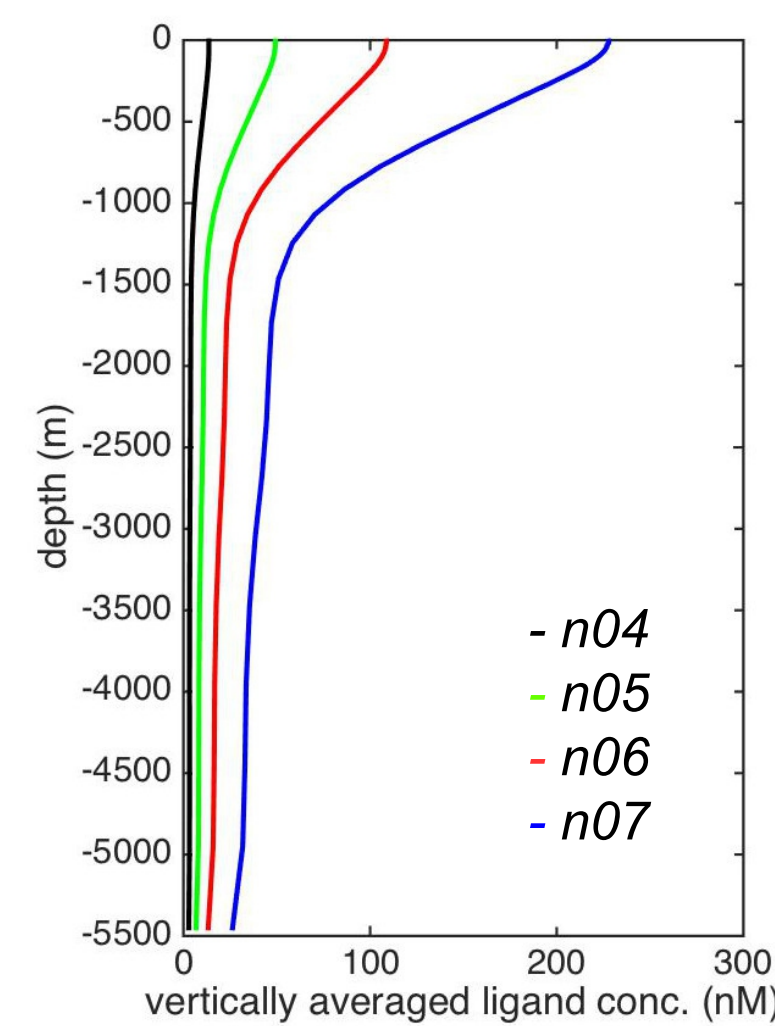


Fig. 2 Vertically averaged ligands of Run n04 – n07.

## II. Changing the $k_{ph}$ ratio

Increasing the photochemical degradation rate decreases ligand concentration throughout the water column with the largest change at the surface in the subtropical regions (Fig. 3a). The modelled surface distribution fits observations a little better, resulting from the more differentiated distribution of ligands. Faster photodegradation leads to a strong decrease in the deep Atlantic and a moderate one in Southern Ocean, leading to unrealistic inter-basin relationship (Fig. 3b).

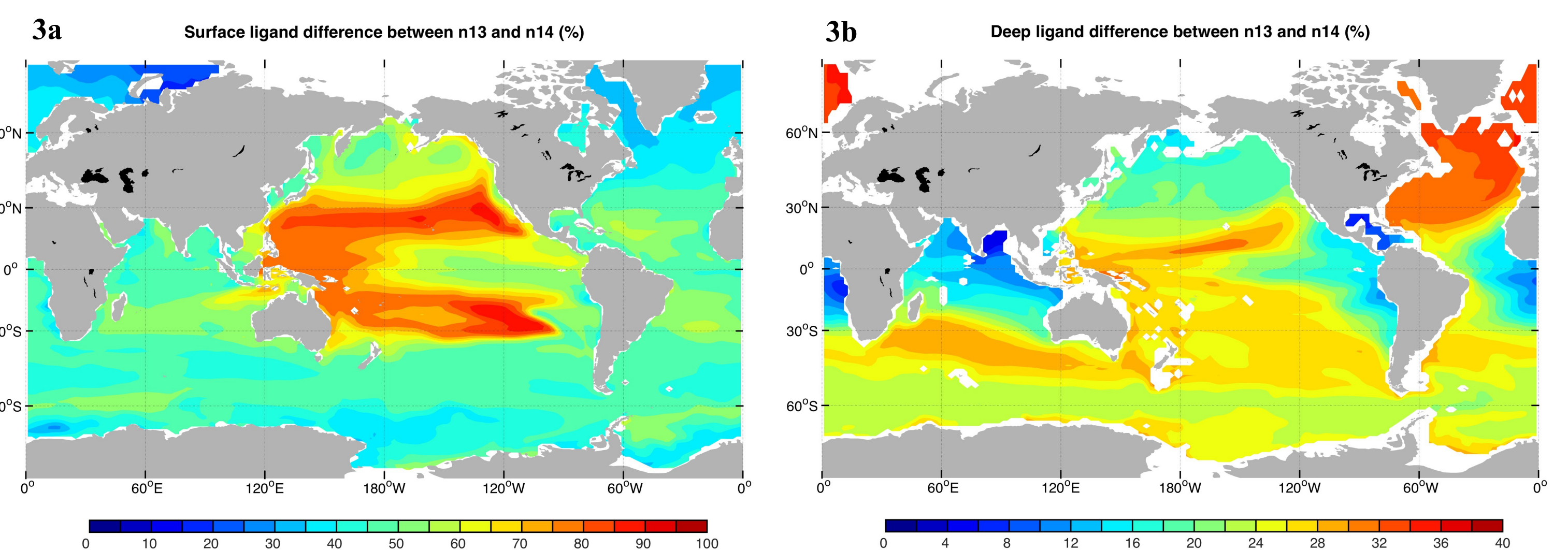
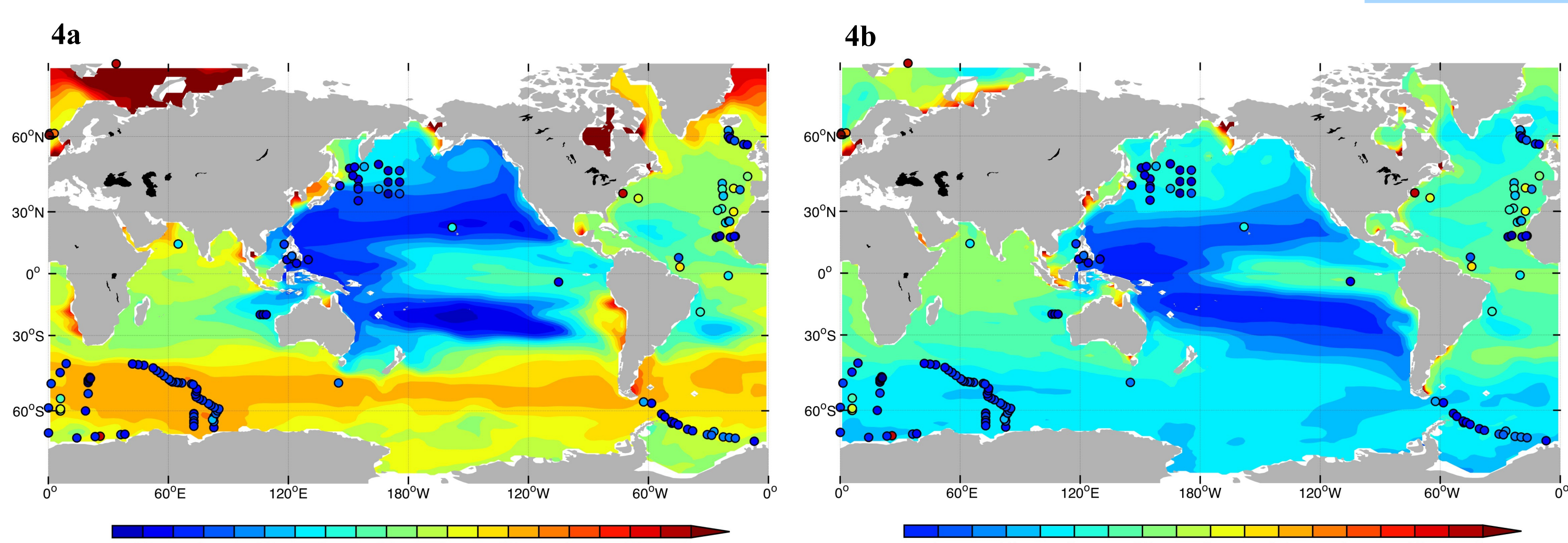


Fig. 3 Difference of ligand concentration between n13 and n14 (%). Colour scalars of the two figures are different.

## III. Changing $\tau$

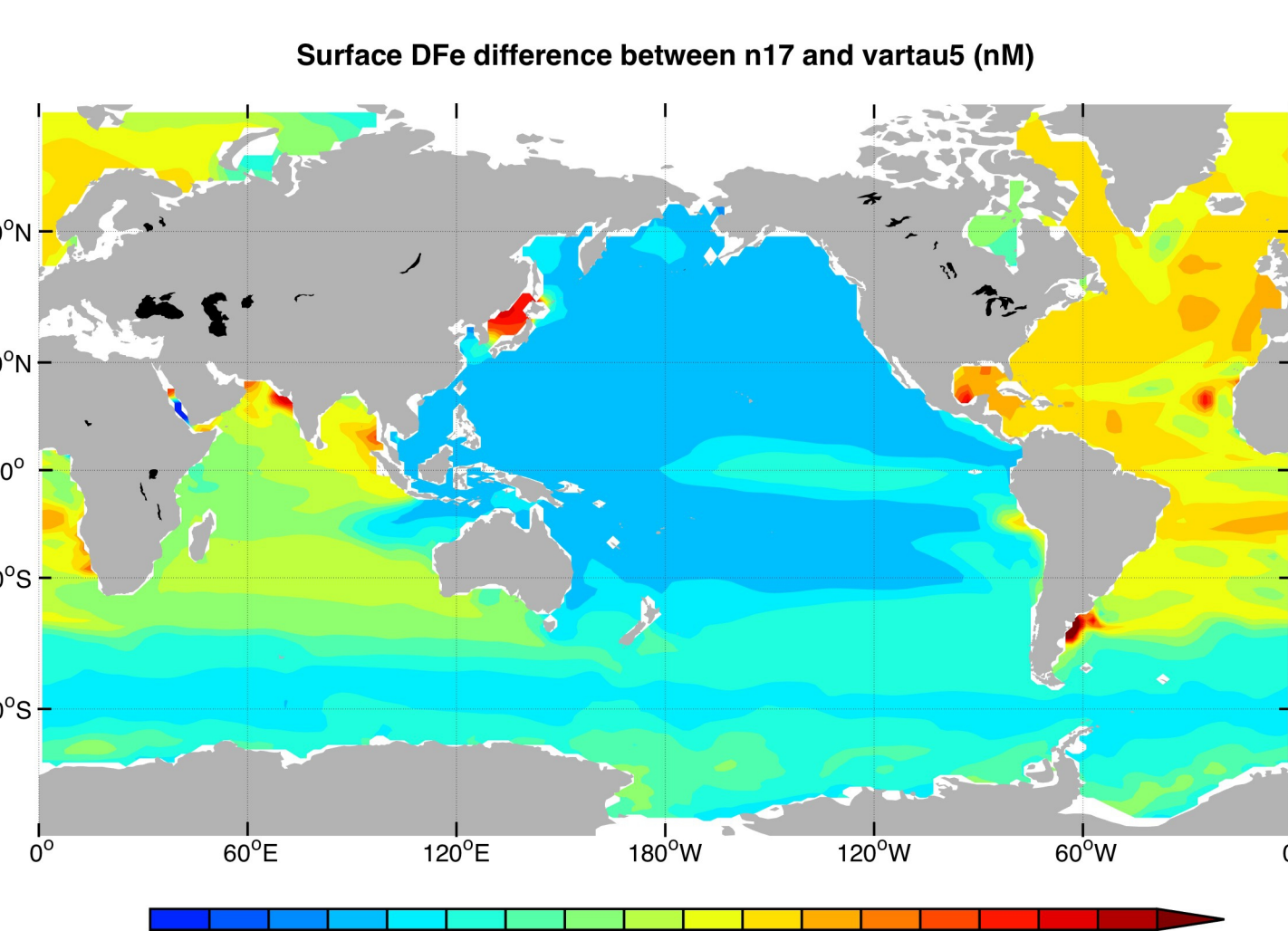
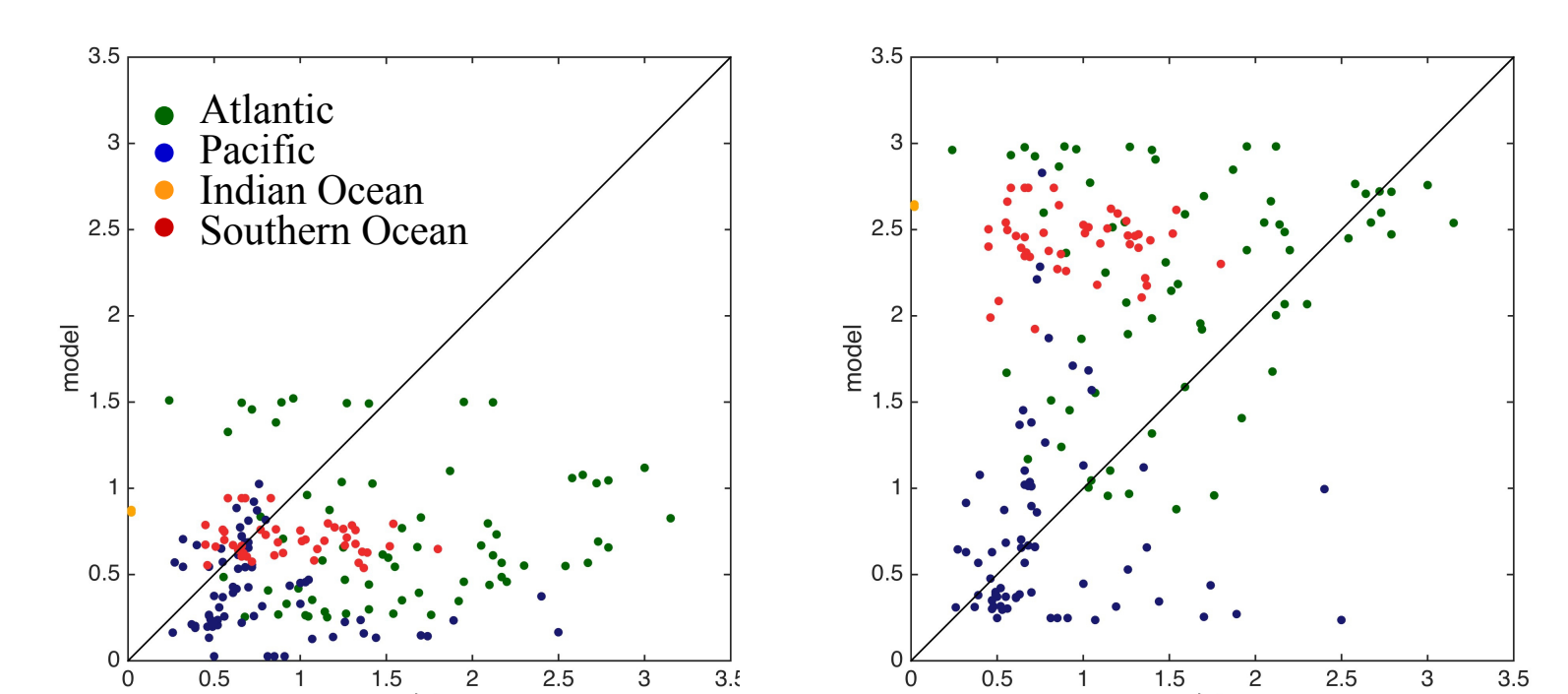
Our model produces unrealistic high ligand concentrations in the Southern Ocean, both at the surface (Fig. 4a) and in the deep ocean, in spite of systematically tuning ligand source and photodegradation. A variable degradation timescale significantly improves the model-data fit in surface waters, particularly moderating the high concentrations in the Southern Ocean and other high latitudes (Fig. 4b).



The deep distribution however shows a poor model-data agreement (Fig.5) in comparison to the run with a degradation timescale of 200 years, indicating that other process might play a role in constraining the inter-basin variability.

Fig. 4a Ligand concentration (nM) in the upper 50 meters in n17; 4b ligand concentration in the upper 50 meters in vartau5. The measured ligand concentrations are shown as coloured circles.

Fig. 5 Model-data comparison of Run vartau5 (left) and n17 (right); ligand concentration (nM) below 1000 meters. Correlation coefficients s. Tab. 1.



Abundance of DFe shows clear feedback to the change of ligand concentration inat the surface with the strongest effect in the North Atlantic, but also in the entire Southern Ocean (Fig. 6). DFe decreases there in a range from 0.2~0.8 nM, which could be critical for this Fe limiting region.

Fig. 6 Difference of surface DFe between runs with fixed and variable microbial degradation timescale (nM).

## Conclusion and outlook

This sensitivity study explored systematically how single processes constrain ligand distribution. This model version with the six processes mentioned above, has not satisfactorily reproduced observed ligand distribution in the global dimension and throughout the water column. Therefore, the model may have to become more complicated, e.g. by a distinction into a more refractory deep ligand pool and a more reactive surface pool, or by introducing a colloidal fraction of ligands into model.